3D Printing of Prototypes Starting from Medical Imaging: a Liver Case Study

Robinson Guachi[1,2[0000-0002-0476-6973]], Michele Bici[1[0000-0002-7744-2152]], Fabiano Bini[1[0000-0002-5641-1189]], Marcelo Esteban Calispa[3[0000-0002-4085-8488]], Cristina Oscullo[2[0000-0001-7622-4922]], Lorena Guachi[2,4[0000-0002-8951-8150]], Francesca Campana[1[0000-0002-6833-8505]] and Franco Marinozzi[1[0000-0002-4872-2980]]

[1] Department of Mechanical and Aerospace Engineering, DIMA – Sapienza University of Rome, 00184, Rome, Italy
[2] Department of Mechatronics, Universidad Internacional del Ecuador - UIDE, 170411, Av. Simón Bolívar, Quito, Ecuador
[3] Department of Mechanical Engineering, Escuela Superior Politécnica de Chimborazo - ESPOCH, 060155, Panamericana Sur km 1 1/2, Riobamba, Ecuador
[4] SDAS Research Group (www.sdas-group.com)
roguachigu@uide.edu.ec

Abstract. Hepatic diseases are serious condition worldwide, and several times doctors analyse the situation and elaborates a preoperative planning based exclusively on the medical images, which are a drawback since they only provide a 2D vision and the location of the damaged tissues in the three-dimensional space cannot be easily determined by surgeons. Nowadays, with the advancement of Computer Aided Design (CAD) technologies and image segmentation, a digital liver model can be obtained to help understand the particular medical case; even with the geometric model, a virtual simulation can be elaborated. This work is divided into two phases; the first phase involves a workflow to create a liver geometrical model from medical images. Whereas the second phase provides a methodology to achieve liver prototype, using the technique of fused deposition modelling (FDM). The two stages determine and evaluate the most influencing parameters to make this design repeatable in different hepatic diseases. The reported case study provides a valuable method for optimizing preoperative plans for liver disease. In addition, the prototype built with additive manufacturing will allow the new doctors to speed up their learning curve, since they can manipulate the real geometry of the patient's liver with their hands.

Keywords: Image segmentation, Convolutional Neural Network, 3D printing, FDM, Liver disease.

1   Introduction

In 2017, the number of adults diagnosed with liver disease was, approximately 4.5 million in USA [1], that means that 1.8% of adults have been diagnosed with liver disease. In many cases, surgery is a procedure widely used for facing a variety of liver pathologies [2]. In selected patients, the advent of new technologies, novel neo-adjuvant

methods and liver regenerative properties have permitted effective resection. Although alternative techniques as percutaneous and laparoscopic procedures have been developed, enhanced and implemented over the past few years; liver surgery is still a complex operation involving a high mortality rate and risk of morbidity. [3-5]. Surgical training and preoperative planning are required for liver surgery, particularly when minimally invasive surgery (MIS) procedures are involved, since the liver tissues of interest in MIS are not directly visualized by the surgeon during the procedures. Preoperative planning (based on 3D virtual models or rapid prototypes) plays an important role in understanding the liver's complex anatomical structure, identifying the damaged areas, determining the best path to insert the instruments while minimizing risk and thereby preserving the liver's functions. [4,6,7].

Medical images from Computed Tomography (CT) and Magnetic Resonance Imaging (MRI) have been used in recent years as a valuable method for anatomical liver structure identification [4,8], medical diagnosis and preoperative planning. But interpreting medical images is often a challenging task and needs specific skills and clinical experience. For this reason, some works in medical field have been done to support the work of the doctors. Therefore, several improvements were made, as proposed in [9-12], to identify, segment or classify the various tissues in healthy, diseased, benign or malignant tumoral. Nevertheless, the images are presented in 2D format, making difficult to distinguish tissues and organs involved. 3D modelling has become a modern toolkit for diagnosis, surgical tool design, preoperative planning, surgical training and simulation of surgical procedures with the use of enhanced medical images through the advancement of computational tools and CAD systems. A 3D geometrical model of anatomical structures obtained from medical images of patients provides details and highlights the location and distance between the organs and the different tissue. Using the additive manufacturing process (3D printing), the 3D geometric model can also be transferred from a virtual environment to a physical environment [13,14]. Applications with silicone material and printable elastomers may also reproduce physical perception of the biological material. Different colours may increase the recognition of different elements (e.g., vascularization of an organ). Moreover, changing the 3D printing filling structure different levels of stiffness may be reproduced.

With the rapid diffusion and easy access to 3D printing desktop systems, prototypes of the 3D models can be obtained with low cost, with good accuracy and in a relatively short time [15]. This paper reports the fundamental set-up and the key aspects of 3D printing via a desktop system, for free shapes derived from Digital Imaging and Communications in Medicine (DICOM). According to the aim, Section 2 outlines a general workflow to obtain a prototype from medical images by 3D printing technology; Section 3 shows the experimental results considering the set-up previously. The results are discussed in Section 4 and, finally, conclusions are outlined in Section 5.

2 Workflow for Printing Patient-Specific 3D Model

Virtual geometrical models have become very helpful tools in the medical field. In Virtual simulations, Finite Element Analysis (FEA) is used to reproduce the interaction

among surgical instruments and soft tissues (organs) [16,17]. In addition, according to unique patient requirements, virtual simulations can be used as a tool to design new instruments. In Virtual surgery, it allows using realistic anatomical models to evaluate and simulate different surgical plans [18]. This procedure is often considered to be a tele-surgery simulator.

With 3D printing processes, [6,13,14], the realistic geometric model could help in identifying zone with diseases for surgery planning and also in improving manual skills during surgery. There is not a general workflow to obtain an accurate geometrical model so far, this document provides our experience with the creation of a patient-specific liver geometric model implemented in a case study, and the procedure is depicted in Fig. 1.
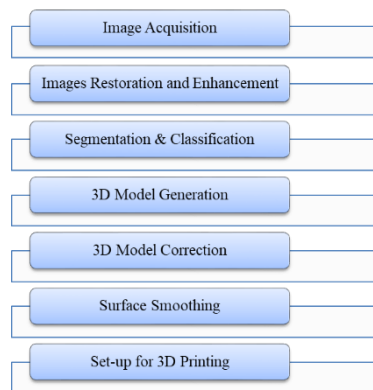

Fig. 1. Workflow for printing patient-specific 3D models.

Image acquisition allows to create a visual representation of inner organs, bones and soft tissues. The most common techniques are the Magnetic Resonance Imaging (MRI), Ultrasound, and Computed Tomography (CT). Different techniques are applied depending on the internal area of interest, the interested tissues and the desired accuracy. The images are saved in the standard format called Digital Imaging and Communications in Medicine (DICOM) for the communication and management of medical imaging information and related data.

Pre-processing of the images, done through *Image Restoration and Enhancements*, facilitates the digitalization of the 3D models and it is also widely used to increase the automatic machine perception, avoiding image defects that may increase difficulties of understanding. Techniques used in image acquisition present some drawbacks due to the noise presence and to the equipment's own configuration. For this reason, pre-processing of the medical images should be done to recover image information from images degraded by noise and blur.

Segmentation and Classification aim at distinguishing objects of interest such as organs, cells, tissues, pathologies, among others, from background pixels. An effective segmentation extracts the shapes with their respective borderlines from the objects of

interest present in an input sequence. Several semi-automatic and automatic methods exist for tissue segmentation purposes. Some software tools such as 3DSlicer, Mimics, Amira are available to perform semi-automatic segmentation, where the ability to accurately segment an image is restricted to the choice of an accurate threshold. The semi-automatic process is often a time-consuming task, particularly if the boundaries are not clearly defined, and the process should therefore be carried out slice by slice. On the other hand, several approaches based on mathematical and theoretical concepts, such as fuzzy logic, genetic algorithms, artificial neural networks, clustering, and so on, have been introduced to automatically perform a segmentation [21-25].

3D Model Generation concerns with surface modeling from the point cloud derived. It can be done interactively or in a semi-automatic way via STL tessellation. Although the segmentation process has been improved, the created 3D model may still have problems, thus *3D Model Correction* may be necessary. STL tessellation uses several connected triangles that correspond to a representation of a solid model's surface geometry, but in the 3D model generation process, commonly some triangles result missing. The typical task performed to correct the actual problems in the geometrical model, includes the following: a) Correct the triangles that are pointed; b) Remove overlapping triangles; c) Fill the missing holes or triangles; d) Rectify the inverted normal; e) Rectify bad edges (bad contours, near edges); f) Re-mesh process, g) Create a single shell (tessellation). It is also necessary to consider during the holes correction process if the hole is a: hole normal, hole ruled, hole freeform or whether it is a bridge in order to obtain a regular and continuous geometry.

The *Surface Smoothing* process is a flexible task meaning that this step can be performed before or after the "3D model correction". It is anyway necessary to conduct an optimization and smoothing process to correct some sharp areas. The optimization increases the number of triangles, the smoothing process reduces irregularities.

Finally, the *Set-up of the 3D Printing* includes the selection of the process parameters to print the STL model. Among different additive manufacturing techniques, the Fused Deposition Modelling (FDM) is currently the most widely used technology, so that it is considered a domestic desktop system for its easy access. This technique uses thermoplastic polymers as a raw material.

3   Case Study

The case study applies the workflow to print a liver disease taken from CT images. They are taken from [19] and represent medical images a liver belonging to woman born in 1987 (Fig. 2).
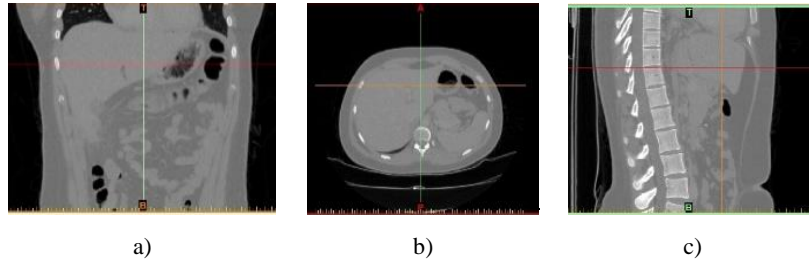
Fig. 2. CT medical images: a) coronal view b) axial view and c) sagittal view.

Image restoration and enhancement were made to reduce blur. It adopts a bicubic interpolator to obtain a smoother surface. It determines the colour value of the pixel through the 16 closest pixels to the input coordinate. Then, the blur kernel is estimated by modelling statistical irregularities in the power spectrum of blurred natural images [10]. Then, the deconvolution process is performed adjusting the blur kernel employing a fast total variation deconvolution FTVd (Fast Total Variation deconvolution) method [20]. After deconvolution process, a sharpening filter is used to mitigate the smoothest, to enhance the borders and to obtain an image free of impulsive noise. Then, histogram equalization is performed to increase the global contrast of the given image and to distribute the intensities on the histogram for getting a contrast-enhanced image. Finally, two erosions and one dilation with a structure of 5x5 are done in order to separate the liver tissues from the rest of the tissues.

Image Segmentation and Classification has been approached by Convolutional Neural Networks (CNNs), since they have gained the ability to successfully support applications in pattern recognition, computer vision, and artificial intelligence. More in details, it has been adopted to explore the ability of CNNs to automatically distinguish the liver (foreground) from no liver (background) pixels [9] to facilitate the development of accurate 3D geometric models. To predict the probability that a pixel might be part of the liver tissues, the proposed approach first splits each image into patches of 28x28 centred on each pixel. Then, each patch is classified through a CNN. Finally, classified patched are arranged to obtain the final segmented image. The general workflow is depicted in Fig. 3.
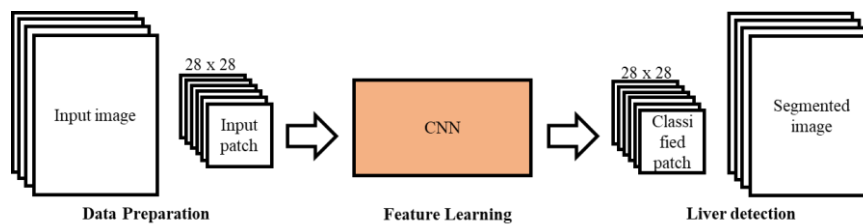

Fig. 3. Scheme of the segmentation approach.

Prior to liver tissues segmentation, 80% of the grayscale slices of CT liver images (each CT image has approximately 1600 slices) are pre-processed to generate a dataset of patches that learns the CNN. Dataset preparation uses ground truth images manually labelled by the operator to assign the corresponding label value to input image patches (1 if the central pixel belongs to the liver tissues, 2 if the central pixel belongs to cancer tissues, otherwise 0). After obtaining the set of patches, LMDB dataset file is generated to be used as input to the CNN, considering that LMDB is a compressed format for working with large dataset. The CNN was implemented starting with a convolutional layer, where each patch is convolved with 20 learnable filters of size 5x5. After that, a down-sampling is performed, through a pooling layer of size 2x2 with a stride of 2 to reduce the spatial size of representation to 25% of its previous size. Then, a convolutional and pooling layer with 50 filters are used. At the end, two fully connected layers with 500 and 3 neurons, respectively act as patch classifier. The outputs from the convolutional and pooling layers represent the high-level features of the input patches, and the fully connected layers use these characteristics to classify the input patch into different classes/labels based on the training dataset. The details of the CNN architecture and its training parameters are depicted in Table 1.

Table 1. CNN architecture and settings for liver segmentation.

Structure	Training Parameters
Input: n patches of size 28×28	Weights were initialized randomly
Conv1: 20 filters of size 5×5	mini-batch of size 128 training sample patches
Pool1: 20 filters of size 2×2	43×10^3 iterations
Conv2: 50 filters of size 5×5	
Pool2: 50 filters of size 2×2	
Fc3: 500 neurons	
Output: 3 neurons	

Deep learning framework CAFFE was used for training purposes. It allows to process data that comes from in normal image format (.jpg, .png, and so on) and LMDB format. The Fig. 4 shows the liver tissues (white pixels) isolated from another soft tissues and background (black pixels). Preliminary results reached an accuracy value of 91% referring to the ground truths manually generated by an expert for experimental purposes.

Fig. 4. Liver tissues classification.

After the application of the CNN, the images belonging to liver (mask) are imported for building the 3D model. Automatic interpolation of segmented images (mask) was made using Mimics. Then the 3D model is generated as an STL file. The 3D model correction has been done through an "Adaptive Re-mesh" with a target triangle edge length of 2 mm, followed by a "Uniform Re-mesh" with a target triangle edge length of 2 mm. Figure 5 shows the 3D final model (Fig. 5a) and before starting the correction (Fig. 5b).
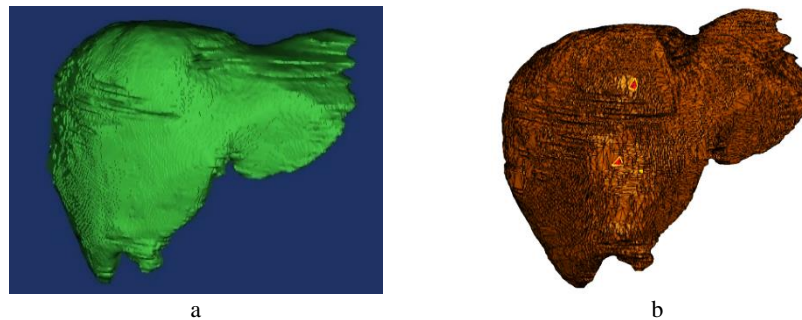

a   b

Fig. 5. a) Liver 3D model; b) Liver geometrical model before correction.

Surface smoothing, shown in Fig. 6a, has been applied on the corrected tessellation with a uniform mesh of 2 mm, a smoothing factor of 0.7 (3 iterations). Local smoothing can be applied only to the area of interest (smaller area with tumoral portion on the case being tested) to avoid an increase in the above-mentioned resolution in areas where it does not offer additional benefits to the presented case study.
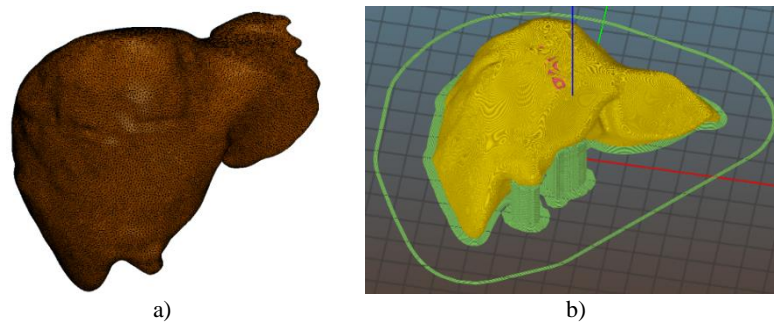

a)   b)

Fig. 6. a) Liver geometrical model for printing; b) Liver geometrical model with the configuration of table 2 into Slic3r.

The liver geometrical model has been built using a FDM device, "TEVO Delta Little Monster" that uses an open source Smoothieboard clone, raw material brown PLA filament (polylactic acid or polylactide) with a diameter of 1.75mm. The path (G-code) for depositing the melted material has been determined using the open source Slic3r software (Fig. 6b). Table 2 displays the parameters considered for the printing of the geometric model of the liver, which were set to obtain a reliable printed model.

Table 2. Parameter to print using Slic3r software.

Parameter	Description
Scale of liver geometrical model	0.5
First layer height	0.2 mm.
Layer height	0.1618 mm.
Perimeters	4
Solid layer top / bottom	4
Infill density	15%
Infill pattern	3D Honeycomb
Top/bottom fill pattern	Concentric
Skirt	Loops:4; Distance from object: 20mm; Skirt height: 1 layer
Brim	4 mm.
Support material/ Overhang threshold	45°
Speed for perimeters	70 mm/s
Speed for small perimeters	25%
Speed for external perimeters	40 mm/s
Speed for infill	120 mm/s
Speed for support material	80 mm/s
Speed for bridges	80 mm/s
Speed for non-print moves	650 mm/s
Temperature extruder	First layer: 230°C; Other layers: 215°C
Temperature Bed	First layer: 80°C; Other layers: 55°C
Diameter filament	1.75 mm.

4   Results and Discussion

Fig. 7 shows half liver with a scale of 0.5 obtained with the parameters described previously. The geometric model has a good surface finish and can illustrate the main characteristics and region of interest of the liver (tumour) as highlighted in Fig. 7. To reduce printing time, the liver was split into two halves.

With the configuration presented in the previous section, the warping effect was reduced, and the support structure was easily removed. Warping effect is a common defect in the FDM technique. It is generated when the printing process goes forward and during the solidification process the previous layer extruded cools. As each region of the printed model cools at different temperature rates, its dimensions change at different rates as well (contraction). Internal stress is therefore produced as a result of the above-mentioned phenomena, and the final effect is to pull the underlying layer upwards (warping).
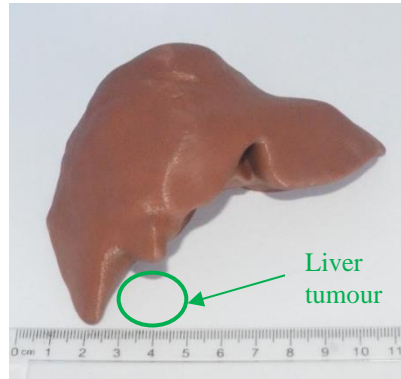
Fig. 7. Liver geometric prototype with the configuration of Table 2 in Slic3r.

To prevent the issue of warping, it is crucial to control the print temperature and increase the adhesion between the print bed and the printed geometric model, therefore, in the test case, the parameter 'Brim' was set to 4 mm in order to create additional (external) loops on the first layer of the printed geometric model. This arrangement improves the adhesion of the printed model to the print bed.

For geometric models with irregular shapes (free form), support structures for the overhang portions must be generated, otherwise the overhang areas or bridges cannot be printed. In this work, the "overhang threshold" parameter has therefore been set to 45°. In the medical field, a good accuracy of the printed model is required, but the time taken to produce a printed model also plays an important role. The 15 percent infill (minimum possible) combined with a 3D honeycomb pattern ensured that the structure does not collapse. The external finishing was more significant in the case study established in this paper, so the speed of the infill and the inner perimeter were set at 120 mm/s and 70 mm/s, respectively, while the speed for external perimeters was set at 40 mm/s.

In accordance with these reasonings and parameters, the final result of the two halves was remarkable, confirming the good accuracy the author found in [15] in another test case. The final prototype, although suffered from the precision of the mounting of the two halves, that could be reduced designing specific pins for insertion and closing, confirmed its good usability for 3D assessing of the medical problem. Although FDM with PLA does not mimic biological deformation at all, it can economically solve the problem of the 3D perception of the disease, aiding the mentoring process at school and the medical preliminary assessment.

5   Conclusions

This work introduces and applies set-up rules for a workflow suitable to build a 3D liver model integrating 2D image segmentation based on CNNs and FDM technique. The output of the CNN is therefore a binary mask where the pixels are recognized and divided into two different classes (liver and background pixels).

The FDM technique provides a good trade-off between quality and time, in addition, the FDM is a low-cost alternative to generate prototypes to help the doctor establish preoperative planning. However, prototypes with the same mechanical properties of liver tissues cannot be created by the FDM system, which may be a drawback when the prototype is used for training new surgeons. Nevertheless, it can economically solve the problem of the 3D perception of the disease, aiding the mentoring process at school and the medical preliminary assessment.

To prevent certain impurities from occurring in the final printed model, it is recommended to consider the 'Skirt' parameter that is useful for cleaning the nozzle before beginning model printing. In cases where, given the complex free-form surfaces, the half liver can be printed, the orientation of the slice should be done in such a way that less structural support can be generated to improve the quality of the finished surface. This consideration prevents potential fractures or other problems when the support structures are detached.

Currently, to improve and continue the development of this research, feasibility analyses and studies are focused on the usage of flexible 3D printable elastomers and also on the design of compliant structure that integrated into the prototype can simulate the behaviour of the organ in terms of deformation.

References

1. U.S. National Library of Medicine, "MedlinePlus," Liver Diseases, 2019. [Online], https://medlineplus.gov/liverdiseases.html#cat_79, last accessed 2021/04/11.
2. Billingsley, K.G., Jarnagin, W.R., Fong, Y., Blumgart, L.H.: Segment-oriented hepatic resection in the management of malignant neoplasms of the liver. Journal of the American College of Surgeons 187(5), 471–481 (1998).
3. McColl, R.J., Shaheen, A.A.M., Brar, B., Kaplan, G., Myers, R., Sutherland, F., Dixon, E.: Survival after hepatic resection: impact of surgeon training on long-term outcome. Canadian Journal of Surgery 56(4), 256–62 (2013).
4. Catalano, O.A., Singh, A.H., Uppot, R.N., Hahn, P.F., Ferrone, C.R., Sahani, D.V.: Vascular and Biliary Variants in the Liver: Implications for Liver Surgery. Radiographics 28(2), 359–378 (2008).
5. Helling, T.S.: Liver failure following partial hepatectomy. HPB 8(3), 165–174 (2006).
6. Ikegami, T., Maehara, Y.: Transplantation: 3D printing of the liver in living donor liver transplantation. Nature reviews Gastroenterology & hepatology 10 (12), 697–698 (2013).
7. Zein, N.N., Hanouneh, I.A., Bishop, P.D., Samaan, M., Eghtesad, B., Quintini, C., Miller, C., Yerian, L., Klatte, R.: Three-dimensional print of a liver for preoperative planning in living donor liver transplantation. Liver Transplantation 19(12), 1304–1310 (2013).
8. House, M.G., Ito, H., Gönen, M., Fong, Y., Allen, P.J., DeMatteo, R.P., Brennan, M.F., Blumgart, L.H., Jarnagin, W.R., D'Angelica, M.I.: Survival after Hepatic Resection for Metastatic Colorectal Cancer: Trends in Outcomes for 1,600 Patients during Two Decades at a Single Institution. Journal of the American College of Surgeons 210(5), 744–752 (2010).
9. Guachi, L., Guachi, R., Bini, F., Marinozzi, F.: Automatic Colorectal Segmentation with Convolutional Neural Network. Computer-Aided Design and Applications 16(5), 836-845 (2019).
10. Kim, S., Lim, H: Method of background subtraction for medical image segmentation, In: CITSA 2006 - 3rd Int. Conf. on Cybernetics and Information Technology, Systems and

Applications jointly with the 4th Int. Conf. on Computing, Communications and Control Technologies, CCCT 2006 - Proc., 1, pp. 87-91. (2006).

11. Gayathri Devi, K., Radhakrishnan, R.: Automatic segmentation of colon in 3D CT images and removal of opacified fluid using cascade feed forward neural network. Computational and Mathematical Methods in Medicine 2015(670739), (2015).

12. Kainz, P., Pfeiffer, M., Urschler, M.: Semantic Segmentation of Colon Glands with Deep Convolutional Neural Networks and Total Variation Segmentation. ArXiv, 1–15 (2015).

13. Uccheddu, F., Carfagni, M., Governi, L., Furferi, R., Volpe, Y., Nocerino, E.: 3D printing of cardiac structures from medical images: an overview of methods and interactive tools. International Journal on Interactive Design and Manufacturing 12(2), 597-609 (2018).

14. Madurska, M.J., Poyade, M., Eason, D., Rea, P., Watson, A.J.M.: Development of a Patient-Specific 3D-Printed Liver Model for Preoperative Planning. Surgical Innovation 24(2), 145-150 (2017).

15. Bici, M., Cardini, V., Eugeni, M., Guachi, R., Bini, F., Campana, F., Marinozzi, F., Gaudenzi, P.: Digital Design of Medical Replicas via Desktop Systems: Shape Evaluation of Colon Parts. Journal of Healthcare Engineering 2018(3272596), (2018).

16. Guachi, R., Bici, M., Guachi, L., Campana, F., Bini, F., Marinozzi, F.: Geometrical modelling effects on FEA of colorectal surgery. Computer-Aided Design and Applications 16(4), 778-788 (2019).

17. Guachi, R., Bini, F., Bici, M., Campana, F., Marinozzi, F., Guachi, L.: Finite element analysis in colorectal surgery: non-linear effects induced by material model and geometry. Computer Methods in Biomechanics and Biomedical Engineering: Imaging and Visualization 8(2), 219-230 (2020).

18. Kühnapfel, U.G., Kuhn, Ch., Hübner, M., Krumm, H.-G., Maass, H., Neisius, B.: The Karlsruhe Endoscopic Surgery Trainer as an example for virtual reality in medical education. Minimally Invasive Therapy and Allied Technologies 6(2), 122-125 (1997).

19. Ircad, 3D-IRCADb-01 database [Online], https://www.ircad.fr/research/3d-ircadb-01/, last accessed 2021/04/11.

20. Yu, H., Huang, T.-Z., Deng, L.-J., Zhao, X.-L.: Super-resolution via a fast deconvolution with kernel estimation. Eurasip Journal on Image and Video Processing 2017(1), art. no. 3 (2016).

21. Christinal, H.A., Díaz-Pernil, D., Jurado, P.R.: Segmentation in 2D and 3D image using tissue-like P system. Lecture Notes in Computer Science (including subseries Lecture Notes in Artificial Intelligence and Lecture Notes in Bioinformatics), 5856 LNCS, 169-176 (2009).

22. Vorontsov, E., Tang, A., Pal, C., Kadoury, S.: Liver lesion segmentation informed by joint liver segmentation. Proceedings - International Symposium on Biomedical Imaging, 2018-April, 1332-1335 (2018).

23. Yang, J., Dvornek, N.C., Zhang, F., Chapiro, J., Lin, M.D., Duncan, J.S.: Unsupervised Domain Adaptation via Disentangled Representations: Application to Cross-Modality Liver Segmentation. Lecture Notes in Computer Science (including subseries Lecture Notes in Artificial Intelligence and Lecture Notes in Bioinformatics), 11765 LNCS, 255-263 (2019).

24. Bici, M., Campana, F., Petriaggi, S., Tito, L.: Study of a Point Cloud Segmentation with Part Type Recognition for Tolerance Inspection of Plastic Components via Reverse Engineering. Computer-Aided Design and Applications 11(6), 640-648 (2014).

25. Bici, M., Campana, F., Trifirò, A., Testani, C.: Development of automatic tolerance inspection through Reverse Engineering. In: 2014 IEEE International Workshop on Metrology for Aerospace, MetroAeroSpace 2014 - Proceedings, art. no. 6865903, pp. 107-112. (2014).